Origin of the maximum in the temperature-dependent electrical resistivity of quasicrystals

2002 J. Phys.: Condens. Matter 14 6975

(http://iopscience.iop.org/0953-8984/14/28/309)

INSTITUTE OF PHYSICS PUBLISHING JOURNAL OF PHYSICS: CONDENSED MATTER

J. Phys.: Condens. Matter **14** (2002) 6975–6988 PII: S0953-8984(02)32394-4

Origin of the maximum in the temperature-dependent electrical resistivity of quasicrystals

J Dolinšek[1], M Klanjšek[1], Z Jagličić[2], A Bilušić[3] and A Smontara[3]

[1] J Stefan Institute, University of Ljubljana, Jamova 39, SI-1000 Ljubljana, Slovenia
[2] Institute of Mathematics, Physics and Mechanics, Jadranska 19, SI-1000 Ljubljana, Slovenia
[3] Institute of Physics, HR-10001 Zagreb, PO Box 304, Croatia

Received 7 January 2002, in final form 3 May 2002
Published 5 July 2002
Online at stacks.iop.org/JPhysCM/14/6975

Abstract

We discuss the origin of the maximum in the electrical resistivity $\rho(T)$ of quasicrystals (QCs) and show that it can be consistently explained as a magnetic effect due to the presence of localized magnetic scattering centres within the quasiperiodic lattice. On the experimental side we present a comparative electrical resistivity–magnetic susceptibility study of icosahedral AlPdMn and CdCa QCs and show correlation between the temperature of the $\rho(T)$ maximum and the electronic paramagnetic magnetization of localized magnetic centres. We propose a theoretical explanation in terms of the Korringa–Gerritsen (KG) model, originally developed for noble metals with diluted transition metal impurities. Unlike the other existing models of electrical conduction in QCs, the KG model describes the $\rho(T)$ maximum as a magnetic effect and predicts its shift to higher temperatures for an increased concentration of magnetic moments.

1. Introduction

The electrical resistivity $\rho(T)$ of quasicrystals (QCs), that generally exhibits a negative temperature coefficient (NTC) on cooling, is one of the most spectacular manifestations of the effect of quasiperiodicity on the physical properties of quasiperiodic metallic alloys. The effect is especially nicely demonstrated in decagonal QCs, where a given sample exhibits an NTC $\rho(T)$ within the quasiperiodic plane, whereas in the orthogonal periodic direction the resistivity is smaller by a factor of several tens and shows a positive temperature coefficient (PTC), as characteristic of regular periodic metals. The mechanism of electrical conduction in QCs has been a matter of intense experimental and theoretical investigation, and has recently been reviewed in several papers [1, 2]. Experiments show that in many cases the conductivity $\sigma = \rho^{-1}$ can be expressed by an empirical form

$$\sigma(T) = \sigma(0) + \Delta\sigma(T), \tag{1}$$

0953-8984/02/286975+14$30.00

where the temperature-dependent part obeys a power law

$$\Delta\sigma(T) \propto T^{\beta}, \tag{2}$$

with $1 < \beta < 1.5$, over a wide temperature range (such as from 4 up to 1000 K). The residual conductivity at low temperature $\sigma(0)$ depends on the composition of the alloy and its structural quality, that depends on the annealing history of the sample. It is worth noting that equation (1) is contradictory to the Matthiessen rule where the T-independent and T-dependent parts of the resistivity, instead of conductivity, are additive.

The conductivities of the icosahedral i-AlPdMn alloys represent a special class where the power law $\Delta\sigma(T) \propto T^{\beta}$ of equation (2) is not obeyed even qualitatively. The i-AlPdMn resistivities $\rho(T)$ in many cases display a maximum [3–8] between room temperature and 4 K, and sometimes in addition a minimum [3, 5, 6] at lower temperatures. The i-AlPdMn family is also special within the Al-based QCs for the strong magnetism of its manganese atoms. The maximum in $\rho(T)$ is not well understood as yet. Quantum interference effects (QIEs) that invoke disorder/quasiperiodicity-induced weak localization (WL) of the extended electronic states provide one possible theoretical explanation. However, there exist several experimental studies [3, 5] that indicate a one-to-one correspondence between the temperature T_m of the $\rho(T)$ maximum and the concentration of the Mn magnetic moments, suggesting that the $\rho(T)$ maximum could be a magnetic effect. It is the purpose of this paper to elaborate further this hypothesis of a magnetic origin of the $\rho(T)$ maximum, from both the experimental and theoretical points of view. From the experimental side we present combined electrical resistivity and magnetic susceptibility measurements of three magnetic i-AlPdMn samples that contain considerably different fractions of magnetic Mn atoms. We then make a comparison with a nominally nonmagnetic binary i-CdCa QC, which, however, also exhibits a maximum in $\rho(T)$ and a significant Curie magnetization at low temperatures due to extrinsic magnetic impurities introduced during sample growth. To explain theoretically the occurrence of the $\rho(T)$ maximum we discuss first the currently available models of electrical conductivity in QCs, namely the variable-range hopping (VRH) conductivity and the QIEs, neither of which take into account magnetic scattering explicitly. Next we show that the maximum in $\rho(T)$ can be consistently explained by the presence of localized magnetic centres in QCs that introduce quasi-bound localized electronic states. We show that this $\rho(T)$ behaviour is not specific to QCs, but is quite commonly found in regular metallic alloys of noble metals (Cu, Ag, Au) with diluted magnetic impurities of transition metals (Mn, Fe) and has been known since the early 1950s [9, 10]. A theoretical description of the $\rho(T)$ maximum has been given by Korringa and Gerritsen [10] (in the following referred to as the KG theory) and it is straightforward to extrapolate their model to QCs, though, at present, on qualitative grounds only. Moreover, the KG theory is not applicable to magnetic QCs only. It also predicts a monotonically increasing NTC resistivity $\rho \propto 1/T$ for nonmagnetic systems where quasi-localized electronic states are formed in the vicinity of nonmagnetic impurities in the host metallic matrix.

2. Experimental results

Before showing our experimental results we discuss briefly two other observations [3, 5] that reported a systematic change of the temperature T_m of the $\rho(T)$ maximum with the Mn concentration in the i-AlPdMn system. Akiyama *et al* [3] have shown that the $\rho(T)$ maximum is formed for Mn concentration between 7 and 10% and T_m is strongly shifted to higher temperatures with increasing Mn concentration. However, these authors did not attribute the appearance of the maximum to the magnetism of the Mn atoms, as they adopted an unphysical assumption that the i-AlPdMn alloys with the Mn concentration lower than 9%

are no longer magnetic. Magnetic measurements [4] have demonstrated that the *i*-AlPdMn QCs exhibit magnetism in the whole icosahedral-phase concentration range (i.e. roughly between 7 and 10% of Mn), but the number of magnetic moments increases strongly with increasing Mn concentration. Another systematic increase of T_m with increasing Mn concentration in *i*-AlPdMn was reported by Rodmar *et al* [5]. Their Czochralsky-grown ingot exhibited a linear gradient of the Mn concentration along the growth direction. Sectioning the ingot into smaller pieces yielded a systematic shift of T_m towards higher temperatures for Mn-richer pieces. As the number of magnetic Mn atoms was reported to be directly proportional to the Mn concentration [4], this suggests a magnetic origin of the $\rho(T)$ maximum. Here it is important that the systematic variation of T_m was observed on pieces of the same sample with a controlled variation of the Mn concentration, so that there is no ambiguity on comparing results of different samples.

Our combined electrical resistivity and magnetic susceptibility measurements were performed on four icosahedral samples, three magnetic *i*-AlPdMn samples with considerably different amounts of magnetic Mn moments and one nominally nonmagnetic *i*-CdCa sample. The first sample, of nominal composition $Al_{72.4}Pd_{20.5}Mn_{7.1}$ (in the following referred to as $AlPdMn_{7.1}$), was monodomain, grown by the Czochralsky method. It was annealed for one day at 800 °C in vacuum. This sample had been used before in NMR diffusion [11], lineshape [12] and relaxation studies [13, 14]. The second sample, of composition $Al_{70.5}Pd_{21.2}Mn_{8.3}$ (referred to as $AlPdMn_{8.3}$), was also Czochralsky grown and monodomain. This sample was 'superannealed' for 35 days at 800 °C in vacuum in order to obtain a structure as perfect as possible. As we show later, the superannealed sample contains a considerably smaller number of magnetic Mn atoms, despite its larger nominal Mn concentration. The third sample, of composition $Al_{72}Pd_{19.5}Mn_{8.5}$ (referred to as $AlPdMn_{8.5}$), was polygrain and its annealing history was not known. As shown later, this sample contains a much larger magnetic Mn fraction than the other two. In addition, the ^{27}Al NMR spin–lattice relaxation rate of this sample (to be shown elsewhere) obeys the Korringa relation $T_1T = \text{const}$, demonstrating its strong metallic character. Both these features—the large magnetic Mn fraction and the strong metallic character—indicate that the $AlPdMn_{8.5}$ sample is not of high quality. The fourth sample was polygrain icosahedral $Cd_{85}Ca_{15}$ (referred to as $CdCa_{15}$). This sample was prepared by high-frequency induction melting, followed by annealing at 400 °C for 430 h. All resistivity measurements were performed by a standard four-terminal method. Magnetic susceptibility measurements were performed in a Quantum Design SQUID magnetometer equipped with a 5 T magnet.

The resistivities were measured in the interval from room temperature to 4 K and are displayed in figure 1. All resistivities exhibit qualitatively similar temperature dependences, first increasing from room temperature upon cooling and then decreasing at low temperatures after passing a maximum. However, significant quantitative differences exist. The room-temperature resistivity of the $AlPdMn_{7.1}$ sample amounts to $\rho_{285\ K} = 2041\ \mu\Omega$ cm. A shallow maximum is observed around 160 K where $\rho_{160\ K} = 2047\ \mu\Omega$ cm, the total increase from room temperature to 160 K being almost negligible, $(\rho_{160\ K} - \rho_{285\ K})/\rho_{285\ K} = 0.3\%$. Below this temperature $\rho(T)$ decreases to $\rho_{4\ K} = 1768\ \mu\Omega$ cm, thus by 14% of its maximum value.

The superannealed $AlPdMn_{8.3}$ sample shows smaller room-temperature resistivity, $\rho_{300\ K} = 1729\ \mu\Omega$ cm. However, the increase of $\rho(T)$ on cooling is much stronger. $\rho(T)$ reaches a maximum at 60 K where $\rho_{60\ K} = 2317\ \mu\Omega$ cm, the total increase being $(\rho_{60\ K} - \rho_{300\ K})/\rho_{300\ K} = 34\%$. The NTC (the slope) of $\rho(T)$ of the superannealed sample is thus much larger and the temperature of the maximum is shifted to considerably lower temperatures. Below the maximum $\rho(T)$ decreases and reaches $\rho_{4\ K} = 2130\ \mu\Omega$ cm, exhibiting an 8% drop from its maximum value. The $\rho(T)$ curve of the $AlPdMn_{8.3}$ crosses that of $AlPdMn_{7.1}$ at 180 K.

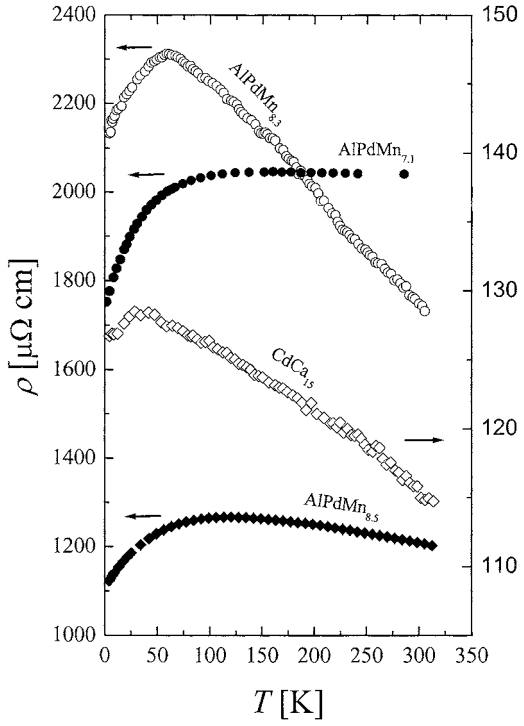

Figure 1. Temperature-dependent electrical resistivities of the four investigated icosahedral quasicrystalline samples: $AlPdMn_{7.1}$ (solid circles), $AlPdMn_{8.3}$ (open circles), $AlPdMn_{8.5}$ (solid diamonds) and $CdCa_{15}$ (open diamonds). The scale on the left applies to the AlPdMn samples whereas the right-hand scale is for the CdCa.

The resistivity of $AlPdMn_{8.5}$ is the smallest among the investigated *i*-AlPdMn samples. Upon cooling it first increases from 1202 $\mu\Omega$ cm at 315 K to 1267 $\mu\Omega$ cm at the temperature of the broad maximum at 120 K, thus by $(\rho_{120\ \mathrm{K}} - \rho_{315\ \mathrm{K}})/\rho_{315\ \mathrm{K}} = 5\%$. Below the maximum $\rho(T)$ decreases to $\rho_{4\ \mathrm{K}} = 1122\ \mu\Omega$ cm, thus by 11% of its maximum value.

The room-temperature resistivity of the $CdCa_{15}$ sample is one order of magnitude smaller and amounts to $\rho_{310\ \mathrm{K}} = 114.5\ \mu\Omega$ cm. Upon cooling $\rho(T)$ reaches a maximum at $T = 30$ K, which is the lowest of all the four investigated samples. The resistivity at the maximum amounts to $\rho_{30\ \mathrm{K}} = 128.5\ \mu\Omega$ cm with the total increase from room temperature $(\rho_{30\ \mathrm{K}} - \rho_{310\ \mathrm{K}})/\rho_{310\ \mathrm{K}} = 12\%$. Below the maximum $\rho(T)$ decreases and reaches $\rho_{4\ \mathrm{K}} = 127\ \mu\Omega$ cm, thus exhibiting a 1% drop from its maximum value.

We present next the magnetic susceptibility $\chi(T)$ measurements of the above four samples in the same temperature range as for $\rho(T)$. Magnetization M was measured in a field $H = 1$ T where the variation of M with H is still linear, so we consider the $\chi = M/H$ ratio in the following. χ contains both a diamagnetic and a paramagnetic contribution, which, in the high-temperature regime, can be described by

$$\chi = \chi_d + \frac{C}{T - \theta}. \tag{3}$$

The diamagnetic contribution was estimated from the room-temperature $\chi(T)$ data. For $AlPdMn_{7.1}$ we obtained $\chi_d = -1.38 \times 10^{-5}$ emu/mol of sample, which is close to the susceptibility $\chi_d \approx -8 \times 10^{-6}$ emu/mol of sample calculated from the tabulated

values of the atomic core diamagnetic susceptibilities. The data were then analysed in the form $(\chi - \chi_d)^{-1}$ versus T. The fit with equation (3) in the high-temperature regime ($T > 50$ K) yielded the Curie–Weiss temperature $\theta = -26$ K and the Curie–Weiss constant $C = 3.2 \times 10^{-2}$ emu K mol^{-1} of Mn, wherefrom we obtain the mean effective moment $p_{eff}^{(\mathrm{exp})} = 0.51\ \mu_B$/(Mn atom). This low $p_{eff}^{(\mathrm{exp})}$ value may be interpreted as an indication that only a fraction f of all Mn atoms carries localized moments. The mean effective moment per magnetic atom in the regime $k_B T \gg p_{eff} H$ is defined as [15] $p_{eff} = p_{eff}^{(\mathrm{exp})}/\sqrt{f}$, so the true mean effective moment p_{eff} is larger than the experimentally measured value $p_{eff}^{(\mathrm{exp})}$ by a factor $1/\sqrt{f}$. For the i-AlPdMn system the actual valence of the Mn atoms is not known, but the p_{eff} values for the three most likely configurations of the Mn ions [16] are all relatively close to 5 μ_B, i.e. $p_{eff}(\mathrm{Mn}^{2+}) = 5.9\ \mu_B$, $p_{eff}(\mathrm{Mn}^{3+}) = 5.0\ \mu_B$ and $p_{eff}(\mathrm{Mn}^{4+}) = 4.0\ \mu_B$. Assuming that the nonzero Mn moments have an average value $p_{eff} \approx 5\ \mu_B$, we derive a fraction $f = (p_{eff}^{(\mathrm{exp})}/p_{eff})^2 = 1.0\%$ of all Mn atoms in the $\mathrm{AlPdMn}_{7.1}$ sample to carry magnetic moments within the analysed temperature range. Our analysis thus interprets the high-temperature susceptibility to indicate that only a small fraction of 1% of all Mn atoms carries localized magnetic moments and that these moments have the full magnitude expected for manganese. Identical analysis was also performed on the $\chi(T)$ data of the $\mathrm{AlPdMn}_{8.3}$ and $\mathrm{AlPdMn}_{8.5}$ samples. For the superannealed $\mathrm{AlPdMn}_{8.3}$ we obtained $p_{eff}^{(\mathrm{exp})} = 0.31\ \mu_B$/(Mn atom), so that a fraction $f = 0.4\%$ of all Mn atoms is magnetic in that sample. This is smaller by a factor of roughly two as compared with $\mathrm{AlPdMn}_{7.1}$. For $\mathrm{AlPdMn}_{8.5}$, on the other hand, we obtained $p_{eff}^{(\mathrm{exp})} = 1.1\ \mu_B$/(Mn atom), yielding a much larger Mn magnetic fraction, $f = 4.8\%$. The small fractions of magnetic Mn atoms of the order of 1% in the investigated $\mathrm{AlPdMn}_{7.1}$ and $\mathrm{AlPdMn}_{8.3}$ samples are consistent with the f values determined from specific-heat and magnetic susceptibility measurements on other good-quality i-AlPdMn samples [17, 18], whereas the large magnetic fraction $f = 4.8\%$ of $\mathrm{AlPdMn}_{8.5}$ is untypical for the i-AlPdMn family, hence indicating its poor structural quality. All paramagnetic susceptibilities are presented in figure 2 in a $\chi - \chi_d$ versus T plot. In order to be comparable to the $\chi(T)$ of the CdCa_{15} sample (also shown in figure 2), the data are given in units of emu/g of sample.

The total susceptibility $\chi(T)$ of the CdCa_{15} sample is displayed as an inset in figure 2. The susceptibility is diamagnetic (negative) and temperature independent down to 30 K, whereas below this temperature a Curie-like upturn is observed. Here care was taken that the contribution of the paramagnetic impurities from the sample holder was subtracted from the total $\chi(T)$, so that the paramagnetic component indeed originates from the CdCa_{15} sample. As neither Cd nor Ca is paramagnetic, the moments can only be of extrinsic origin, introduced into the sample during the growth process. Since we do not know what kind of paramagnetic impurities are contained within the sample, we are not able to perform a quantitative analysis similar to that conducted for the i-AlPdMn samples. However, since the diamagnetic contribution χ_d is well defined, we are able to extract the paramagnetic contribution $\chi - \chi_d$, which, when expressed in the emu/g of sample units, may then be compared with the paramagnetic susceptibilities of the i-AlPdMn samples. This is shown in figure 2, where $\chi - \chi_d$ of all four samples are displayed. The paramagnetic susceptibility of the CdCa_{15} sample is very small as compared with the i-AlPdMn samples.

Comparing now the $\chi(T)$ and the $\rho(T)$ data of each sample, we find the following interesting correlation between the paramagnetic susceptibility and the temperature of the $\rho(T)$ maximum. In the least magnetic sample, CdCa_{15}, the maximum in $\rho(T)$ is observed at 30 K, which coincides with the temperature below which $\chi - \chi_d$ starts to become significant. In $\mathrm{AlPdMn}_{8.3}$ the $\rho(T)$ maximum occurs at 60 K, which is again the temperature below which

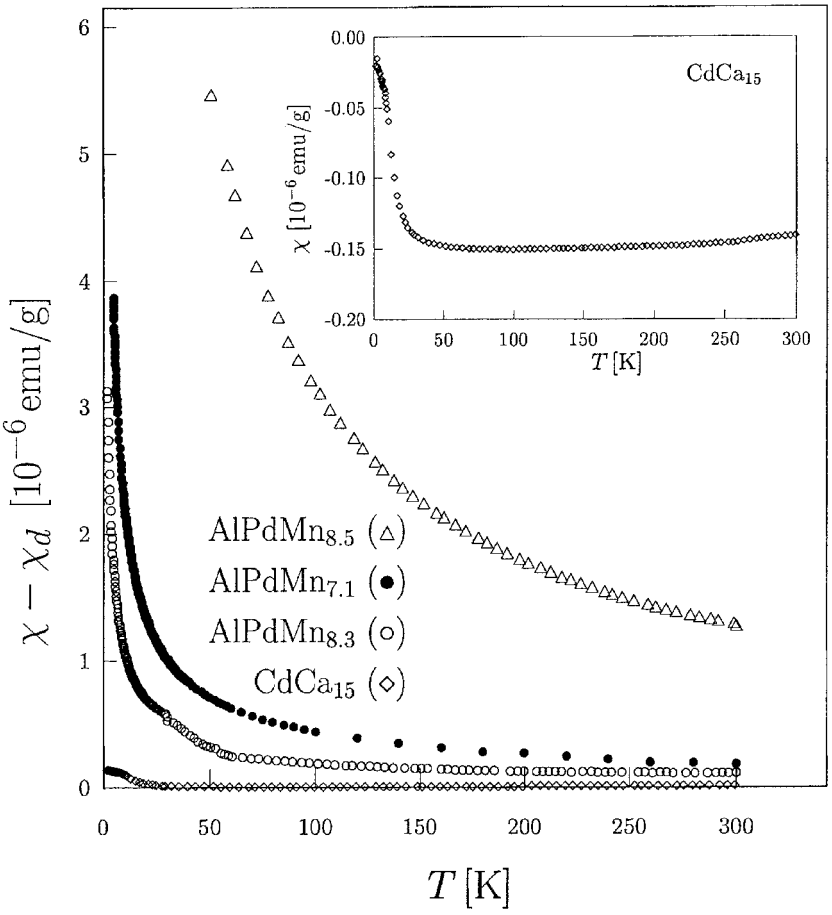

Figure 2. Temperature-dependent paramagnetic susceptibilities $\chi - \chi_d$ of AlPdMn$_{7.1}$ (solid circles), AlPdMn$_{8.3}$ (open circles), AlPdMn$_{8.5}$ (triangles) and CdCa$_{15}$ (diamonds). The inset shows the total susceptibility (diamagnetic plus paramagnetic) of the CdCa$_{15}$ sample.

$\chi - \chi_d$ becomes significant. For AlPdMn$_{7.1}$, there is almost no temperature dependence of $\rho(T)$ above 100 K, but there is a significant decrease below 100 K, which again coincides with the temperature, below which $\chi - \chi_d$ becomes large. A similar conclusion also can be drawn, at least qualitatively, for AlPdMn$_{8.5}$. This analysis indicates that there exists a correlation between the temperature of the $\rho(T)$ maximum and the magnitude of the paramagnetic susceptibility, supporting the hypothesis of a magnetic origin of the resistivity maximum. It also suggests that the origin of the magnetic moments may not be of crucial importance in this issue. The moments may be either intrinsic to the quasicrystalline structure (like Mn in *i*-AlPdMn or Fe in *i*-AlCuFe) or extrinsic, provided they are more or less randomly distributed within the sample.

3. Discussion

We discuss now the possible origin of the $\rho(T)$ maximum from the theoretical point of view by first considering the currently existing theories of electrical conduction in QCs. Here two different approaches exist. In the first approach the theory of Anderson localization in

disordered metals is extrapolated to QCs, where quasiperiodicity introduces localization of the electronic states, yielding an insulating state at $T = 0$. At nonzero temperatures thermally activated electron hopping (or tunnelling) between localized states drives these states back into conduction, resulting in hopping-type conductivity. The low-temperature conductivity is considered to obey a $\ln \sigma(T) \propto T^{-1/4}$ dependence (the Mott law) or $\ln \sigma(T) \propto T^{-1/2}$ in the case when Coulomb repulsion is included [19]. The resulting resistivity $\rho = \sigma^{-1}$ is monotonically increasing towards $T \to 0$, exhibiting an NTC, but no maximum. It is also not consistent with the experimentally observed power law of equation (2).

A more QC-specific model of the dc conductivity was given by Janot [20, 21] in terms of hierarchically variable-range electron hopping (VRH) between localized states. The VRH model yields an insulating state at $T = 0$, whereas at $T \neq 0$ the number of charge carriers in the conduction band increases as a power law of temperature due to the phonon-assisted excitation over the quasiperiodicity-induced hierarchical sequence of potential barriers. Except close to $T = 0$, the resulting resistivity behaves as $\rho \propto 1/T$, thus predicting a monotonic increase with an NTC on cooling that is consistent with the empirical law of equation (2) (with $\beta = 1$). However, the VRH theory again does not predict a maximum in $\rho(T)$.

The second approach relies on the QIE. Unlike the hopping conduction that drives localized states back into conduction, QIEs modify contribution of extended states either by modification of the electronic diffusivity (the WL effect) or by inducing changes in the density of states (DOS) at the Fermi level $g(E_F)$ (the *electron–electron interactions*, EEIs). QIEs are important at low temperatures only as thermal vibrations and any inelastic processes destroy interference. QIE terms contribute small corrections to the Boltzmann conductivity and it is a usual practice to write the conductivity in the form of equation (1)

$$\sigma(T) = \sigma(0) + \Delta\sigma_{EEI}(T) + \Delta\sigma_{WL}(T). \tag{4}$$

The EEI term depends on temperature as [22, 23] $\Delta\sigma_{EEI}(T) \propto \sqrt{T}$. The WL contribution includes spin–orbit and inelastic scattering and can be written in the form [22–24]

$$\Delta\sigma_{WL}(T) = A(3\sqrt{t+1} - \sqrt{t} - 3). \tag{5}$$

Here $A = e^2/(2\pi^2\hbar\sqrt{D\tau_{so}})$ with D representing the diffusion constant and τ_{so} the spin–orbit scattering time of the electrons, and $t = \tau_{so}/4\tau_i(T)$, where $\tau_i$is the inelastic scattering time. The last term in equation (5) is usually added to keep $\Delta\sigma_{WL}(T) = 0$ at $T = 0$ [22]. It is considered that the only temperature-dependent quantity in equation (5) is τ_i, which obeys a power law $\tau_i \propto T^{-p}$, at least within a limited temperature range. The exponent p depends on the type of inelastic scattering mechanism (electron–phonon, electron–electron etc) and was predicted [25] to be in the range $1.5 < p < 3$. While $\Delta\sigma_{EEI}(T) \propto \sqrt{T}$ changes with temperature monotonically, $\Delta\sigma_{WL}(T)$ exhibits a minimum (or equivalently the resistivity shows a maximum) for $\tau_{so}/\tau_i(T) = 1/2$. Within the above WL model, the maximum in $\rho(T)$ occurs as a consequence of the crossover from the dominant inelastic scattering at high temperature to a dominant spin–orbit scattering at low temperature, where the strong spin–orbit scattering introduces a kind of re-entrant antilocalization of the electrons at low T. The WL theory thus predicts the maximum in $\rho(T)$ and its NTC above the maximum, but does not consider these effects to be of magnetic origin. In the limit of high temperatures both QIE corrections vanish, i.e. $\Delta\sigma_{EEI}(T) = \Delta\sigma_{WL}(T) = 0$. It was estimated [22] that the EEI contribution in the *i*-AlPdMn probably vanishes in the temperature range 10–50 K, whereas the WL contribution may survive to somewhat higher temperatures, such as 150–200 K. For this reason the fitting of the experimental $\sigma(T)$ curves away from the low-temperature regime with the equation (4) can give quite uncertain results.

The above two approaches—the hopping conduction and the QIE—are both based on the disorder/quasiperiodicity-induced localization of the electronic states and do not take explicitly

into account the scattering of conduction electrons on magnetic centres. However, the clear experimental evidence that the temperature T_m of the $\rho(T)$ maximum in magnetic QCs depends on the concentration of magnetic atoms prompts a different theoretical approach that would

(i) still take into account the localized nature of electronic states, but
(ii) also consider magnetic scattering in an explicit way.

A simple phenomenological theory that includes both these effects is the KG model [10], which was developed in the early 1950s to explain the $\rho(T)$ maximum in regular metallic alloys of noble metals with diluted magnetic impurities of transition metals (Mn, Fe). The theory is in fact more general, describing the resistivity of noble metals containing either magnetic or nonmagnetic transition metal impurities. It is essentially based on the same physical principle as the hopping-conduction and WL theories—the existence of localized electronic states in the vicinity of Fermi level. In the following we give a brief account of the KG theory and discuss its applicability to QCs.

Because of their different valency, diluted transition metal impurities in a host metallic matrix act as a scattering potential to the conduction electrons. The consequence of scattering is a build-up (or depletion) of electronic charge around the impurity that screens the excess nuclear charge. The screening produces a long-range oscillating charge density, known as Friedel oscillations [26]. The KG theory assumes that the screening electrons occupy virtual bound states [27], where the electrons are in localized states, but their energies lie within the conduction band energies. If the impurities are nonmagnetic, the virtual-bound-state energies are centred at the Fermi energy ε_F. When the impurities are magnetic due to unpaired d electrons, the bound-state energies are shifted by the spin energy $\pm\varepsilon_1$ due to the s–d exchange interaction. Each of the two split levels is assumed to have a width Δ, so the bound-state energies lie within the intervals $\varepsilon_F + \varepsilon_1 \pm \Delta/2$ and $\varepsilon_F - \varepsilon_1 \pm \Delta/2$. The scattering mechanism that determines the resistivity may be considered as a process where the incoming conduction electron throws the local electron out of its quasi-bound state by means of Coulomb interaction, and becomes at the same time captured in its place in either the $\varepsilon + \varepsilon_1$ or $\varepsilon - \varepsilon_1$ state, according to its own spin direction. This process may be regarded as a kind of a resonance effect, where the incoming conduction electron has the same energy as the electron in the localized state. The collision time τ for such processes is effectively zero, thus contributing significantly to the resistivity. The occurrence of the maximum in $\rho(T)$ can be understood from the simple 'relaxation-time' formula for the conductivity

$$\sigma = -\left(\frac{e^2 k_F^2}{3\pi^2\hbar^2}\right)\int_{-\infty}^{+\infty}\frac{\mathrm{d}\varepsilon}{\mathrm{d}k}\tau\frac{\mathrm{d}f}{\mathrm{d}\varepsilon}\,\mathrm{d}\varepsilon, \tag{6}$$

where $k = |\vec{k}|$ is the wavevector of the conduction electron, k_F the Fermi wavevector and f the Fermi–Dirac distribution function. The function $\mathrm{d}f/\mathrm{d}\varepsilon$ is a bell-shaped function centred at ε_F with the width proportional to $k_B T$. The temperature dependence of $\rho = \sigma^{-1}$ originates from the assumption that τ varies with energy, $\tau = \tau(\varepsilon)$. In the simplest approximation one takes $\tau \approx 0$ for energies of the quasi-bound states and $\tau \approx \text{const} \neq 0$ elsewhere. At high temperatures the function $\mathrm{d}f/\mathrm{d}\varepsilon$ is broad enough to extend over the quasi-bound energy bands centred at $\varepsilon_F \pm \varepsilon_1$. Upon cooling the width of $\mathrm{d}f/\mathrm{d}\varepsilon$ decreases and the weight of the quasi-bound states becomes increasingly more important in the integral of equation (6), so the resistivity increases. At still lower temperatures, $\mathrm{d}f/\mathrm{d}\varepsilon$ becomes so narrow that it no longer integrates over the quasi-bound energies and the resistivity starts to drop after it has reached a maximum. Upon $T \to 0$, ρ tends to approach the value ρ_0 of a pure metal without impurities, where, within the KG theory, ρ_0 is given by the Drude form $\rho_0^{-1} = ne^2\tau/m$. The above model

yields an expression for the resistivity [10]

$$\left(\frac{\rho}{\rho_0}\right)^{-1} = 1 - \left[\tanh\left(\frac{\varepsilon_1 + \Delta/2}{2k_BT}\right) - \tanh\left(\frac{\varepsilon_1 - \Delta/2}{2k_BT}\right)\right], \tag{7}$$

where the origin of the energy scale was shifted to $\varepsilon_F = 0$. At temperatures $k_BT \gg \Delta$ equation (7) becomes particularly simple,

$$\frac{\rho}{\rho_0} = 1 + \frac{2\Delta}{k_BT}\frac{\exp(\varepsilon_1/k_BT)}{[1+\exp(\varepsilon_1/k_BT)]^2}, \tag{8}$$

predicting a maximum in $\rho(T)$ at a temperature $T_m = 0.65\varepsilon_1/k_B$. In the case of nonmagnetic impurities there is no spin-dependent energy splitting, so the energies of the quasi-bound states are now centred at ε_F with the total width 2Δ. This situation corresponds to placing $\varepsilon_1 = \Delta/2$ into equation (7), yielding

$$\left(\frac{\rho}{\rho_0}\right)^{-1} = 1 - \tanh\left(\frac{\Delta}{2k_BT}\right). \tag{9}$$

Here the resistivity does not exhibit a maximum, but rather increases monotonically towards $T \to 0$, a consequence of the fact that the $\tau \approx 0$ condition is now fulfilled in an energy interval of width 2Δ centred at the Fermi level. In the $k_BT \gg \Delta$ limit, $\rho(T)$ exhibits a simple $1/T$ increase upon cooling

$$\frac{\rho}{\rho_0} = 1 + \frac{\Delta}{2k_BT}. \tag{10}$$

The predictions of the KG theory are thus in qualitative agreement with the experimental $\rho(T)$ curves of QCs, both magnetic and nonmagnetic. For nonmagnetic samples the theory predicts a monotonically increasing NTC resistivity $\rho \propto 1/T$ on cooling, whereas for magnetic samples $\rho(T)$ exhibits a maximum. As the temperature of the maximum is proportional to the exchange energy, $T_m \propto \varepsilon_1$, which for small concentration c of magnetic atoms itself increases as $\varepsilon_1 \propto c$; this also correctly predicts the increase of T_m for more magnetic samples. This $T_m \propto c$ dependence was indeed observed in regular alloys [9, 10] (Cu, Ag, Au)–Mn and Au–Cr, where, in addition, the NTC of $\rho(T)$ at temperatures above the maximum was smaller and the maximum less pronounced for an increasing concentration of Mn(Cr) moments (a similar situation that is also displayed in our figure 1). However, one has to be aware of the limitations of the KG theory. First, the assumption $\tau = \tau(\varepsilon)$ with $\tau \approx 0$ for the quasi-bound states and $\tau \approx$ const elsewhere is purely phenomenological. Second, the theory assumes that the scattering by the 'foreign' atoms is elastic (so the spin does not change). Next the theory is derived for low temperatures where the phononic resistivity can be neglected and for low concentration c of 'foreign' atoms (typically $c < 1$ at.%) such that they can be treated as independent. The resulting temperature-dependent term appears as a small correction to the Drude resistivity, $\rho(T) = \rho_0 + \Delta\rho(T)$, which, however, correctly obeys the Matthiessen rule.

It is interesting to consider to what extent the KG theory can be applied to QCs. Since QCs quite generally exhibit a weak metallic character down to low temperatures, one can anticipate that some extended electron states should exist. On the other hand, it is now widely accepted that in the *i*-AlPdMn-type structure there also exist quasi-localized states, where a fraction of electrons are confined to the basic building blocks of the structure, the pseudo-Mackay icosahedral atomic clusters. It can therefore be anticipated that quasi-bound and extended states coexist in real QCs, in analogy to noble metals with transition impurities. Diluted magnetic impurities exist in magnetic QCs too. In *i*-AlPdMn typically 1% of all Mn atoms are magnetic. Since the total Mn concentration amounts to about 8%, this makes 0.08% of

all atoms in the *i*-AlPdMn structure carry magnetic moments, thus a diluted quantity. In *i*-AlCuFe a fraction 10^{-4} of the total number of Fe atoms are magnetic [6, 28]. These two QC families thus possess both essential properties that lead to the maximum in $\rho(T)$ within the KG theory. In *i*-AlPdMn the maximum in $\rho(T)$ is observed at relatively high temperatures close to 100 K (see [3–6] and the present work), whereas in *i*-AlCuFe [6–8] the maximum is shifted to considerably lower temperatures of about 10 K. This is consistent with the smaller number of magnetic centres in the *i*-AlCuFe samples. The above considerations suggest that it may be a straightforward procedure to apply the KG theory to QCs. The neglect of the phononic contribution to the resistivity can be argued by the fact that phonons generally cannot propagate within the quasiperiodic lattice (except for the long-wavelength acoustic ones). However, due to the fundamental difference between the QCs and the regular metallic alloys with transition metal impurities, one can expect that the KG theory in its original form (equations (7) and (9)) may be applicable to QCs only qualitatively, but may serve as a reasonable starting point towards a more complete, QC-specific theory of electrical resistivity.

It is worth mentioning that an anomalously decreasing resistivity at low temperatures upon cooling due to magnetic effects was also predicted by Yosida [29] and Schmitt [30], who considered magnetic metallic alloys with antiferromagnetically (AFM) coupled moments (e.g. Cu–Mn). Yosida considers a spin-dependent (exchange) plus a spin-independent (screened Coulomb potential around the Mn ions) interaction between conduction 4s electrons and the localized 3d (Mn) electrons in the dilution limit ($c < 1$ at.% of Mn). Both, elastic and inelastic scattering processes are taken into account, whereas lattice vibrations are neglected. The resulting resistivity is temperature independent at high temperatures and starts to decrease gradually on approaching the Néel temperature T_N due to the appearance of short-range AFM order. Below the AFM transition the resistivity continues to drop monotonically. The anomalous decrease of $\rho(T)$ at low temperatures is here a consequence of the s–d exchange interaction, thus of magnetic origin. The theory can explain the T-independent plateau of the resistivity at high temperatures and a monotonic decrease in the regime where short-range AFM correlations set in (that can occur quite high above T_N), but cannot explain the maximum in $\rho(T)$. The theoretical $\rho(T)$ curves are very similar to our experimental curve of the $AlPdMn_{7.1}$ sample displayed in figure 1. Here the Mn moments in $AlPdMn_{7.1}$ are also AFM coupled via indirect exchange, as evidenced from the negative Curie–Weiss temperature $\theta = -26$ K, but there is no AFM phase transition. Further work is needed to elaborate the applicability of the Yosida theory to magnetic QCs.

We now apply the KG theory to the experimental $\rho(T)$ data displayed in figure 1. Since the QIE model offers an alternative explanation of the $\rho(T)$ maximum, we compare in the following theoretical fits of both models on the same graph. For the KG model, the fit was made with equation (7), that involves three fit parameters—the exchange energy ε_1, the width of the quasi-bound states Δ and the residual resistivity ρ_0. The QIE fit, on the other hand, was made with the ansatz $\rho^{-1}(T) = \sigma(0) + \Delta\sigma_{WL}(T)$, with $\Delta\sigma_{WL}$ given by equation (5). This fit involves four fit parameters: $\sigma(0)$, A, p and the temperature T_0. Here T_0 is defined by taking the inelastic scattering time in the form $\tau_i = \tau_i^0/T^p$ and then writing $t = \tau_{so}T^p/(4\tau_i^0) = (T/T_0)^p$, so that $T_0 = (4\tau_i^0/\tau_{so})^{1/p}$.

For the $AlPdMn_{7.1}$ sample (figure 3), the QIE model cannot reproduce the experimental data even qualitatively. This model yields a relatively large NTC resistivity at temperatures above the $\rho(T)$ maximum and is hence not applicable to the resistivities of the type of $AlPdMn_{7.1}$ that exhibit a small NTC (or even a T-independent-like plateau) at high temperatures. As mentioned before, this type of $\rho(T)$ is quite commonly found within the *i*-AlPdMn family. An attempt to make a qualitative fit (solid curve in figure 3) yielded the parameters $\sigma(0) = 5.2 \times 10^{-4}$ $(\mu\Omega\ \mathrm{cm})^{-1}$, $A = 1.73 \times 10^{-4}$ $(\mu\Omega\ \mathrm{cm})^{-1}$, $T_0 = 291$ K and

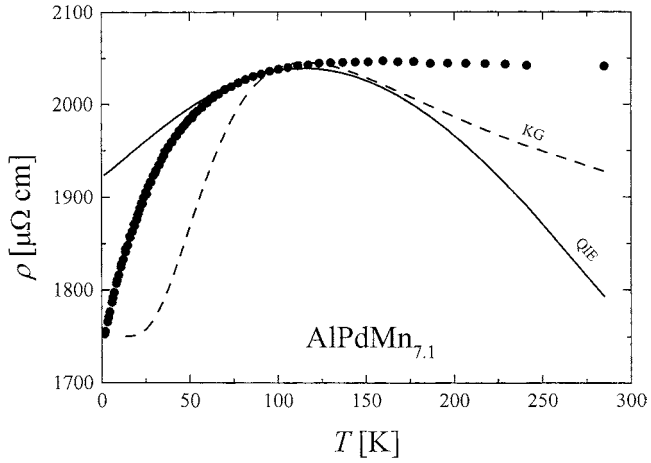

Figure 3. Electrical resistivity of the $AlPdMn_{7.1}$ sample fitted with the QIE model (solid curve) and the KG model (dashed curve). The fit functions and the fit parameters are defined in the text.

$p = 2.23$. The fit fails to reproduce the data at both high and low temperatures, wherefrom we conclude that the QIE model is not applicable in this case. The KG fit is not much better. A qualitative fit (dashed curve in figure 3) was obtained with the fit parameters $\rho_0 = 1750\,\mu\Omega$ cm, $\varepsilon_1 = 180$ K and $\Delta = 58$ K. Neither of the two models thus fits the $\rho(T)$ data of the $AlPdMn_{7.1}$ satisfactorily.

The $\rho(T)$ data of the superannealed $AlPdMn_{8.3}$ sample exhibit a much larger NTC at temperatures above the $\rho(T)$ maximum and the QIE model yields a good fit (solid curve in figure 4) using fit parameters $\sigma(0) = 4.6 \times 10^{-4}$ $(\mu\Omega\ \text{cm})^{-1}$, $A = 1.55 \times 10^{-4}$ $(\mu\Omega\ \text{cm})^{-1}$, $T_0 = 207$ K and $p = 1.66$. The fit reproduces excellently the data from room temperature down to 80 K, whereas below this temperature the fit is less perfect. Here it is astonishing that the fit is excellent at high temperatures, where the QIE theory is considered non-applicable, whereas it is less good at low temperatures, where it should be valid. The KG fit (dashed curve) with fit parameters $\rho_0 = 1842\,\mu\Omega$ cm, $\varepsilon_1 = 88$ K and $\Delta = 40$ K is qualitative only, reproducing the general $\rho(T)$ trend, but not its details. For the $AlPdMn_{8.3}$ sample the QIE fit can be considered as good whereas the KG theory is applicable only qualitatively.

A similar situation is encountered for the $CdCa_{15}$ sample, that again shows a large NTC of $\rho(T)$ in the high-temperature regime. Here the QIE fit (solid curve in figure 5) with the parameters $\sigma(0) = 7.9 \times 10^{-3}$ $(\mu\Omega\ \text{cm})^{-1}$, $A = 6.26 \times 10^{-4}$ $(\mu\Omega\ \text{cm})^{-1}$, $T_0 = 153$ K and $p = 1.50$ is almost perfect (except in the close vicinity of the $\rho(T)$ maximum). The KG fit, on the other hand, is again qualitative only, reproducing the general $\rho(T)$ trend, but fails quantitatively. An indicative fit (dashed curve in figure 5) was made using parameters $\rho_0 = 118\,\mu\Omega$ cm, $\varepsilon_1 = 43$ K and $\Delta = 10$ K.

The $\rho(T)$ curve of $AlPdMn_{8.5}$ is analysed in figure 6. This kind of $\rho(T)$, exhibiting a small NTC above the $\rho(T)$ maximum and a large drop below, is most typical for the *i*-AlPdMn family and is encountered in the majority of the *i*-AlPdMn samples. We show in the following that for the $\rho(T)$ curves of this kind the slightly modified KG theory reproduces the data well, whereas the QIE theory is not applicable. The simple KG fit with equation (7) (dashed curve in figure 6) was obtained with the fit parameters $\rho_0 = 1100\,\mu\Omega$ cm, $\varepsilon_1 = 155$ K and $\Delta = 48$ K. As before, the fit is qualitative and reproduces reasonably the general $\rho(T)$ trend, but not its details. An improved fit could be made by introducing a distribution of the ε_1 parameter that broadens

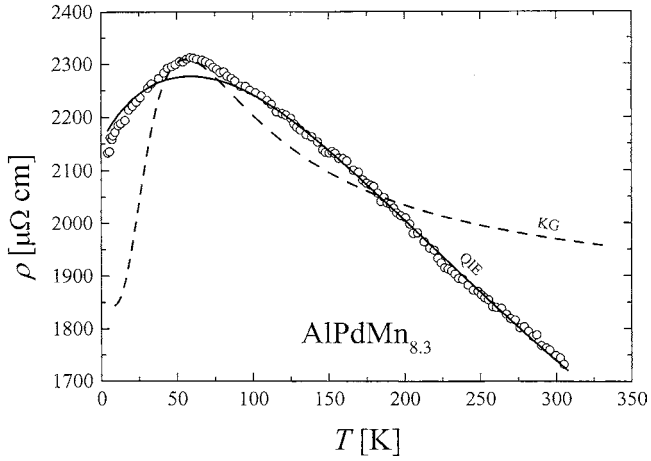

Figure 4. Electrical resistivity of the superannealed $AlPdMn_{8.3}$ sample fitted with the QIE model (solid curve) and the KG model (dashed curve).

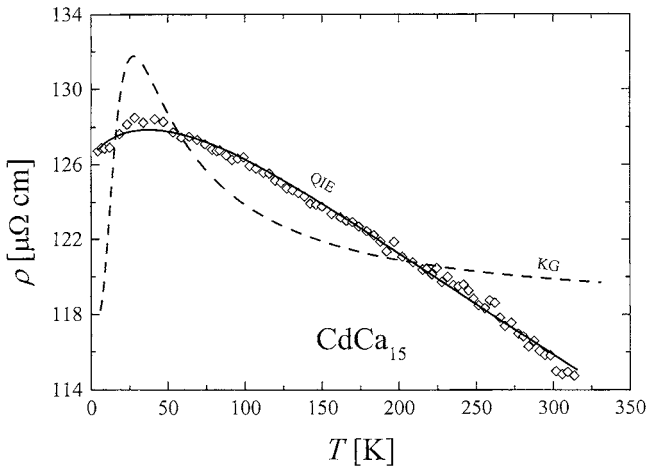

Figure 5. Electrical resistivity of the $CdCa_{15}$ sample fitted with the QIE model (solid curve) and the KG model (dashed curve).

the maximum in $\rho(T)$. Due to the lack of translational periodicity in the QC lattice and the related large manifold of different atomic environments, such a distribution is straightforward to introduce. A fit using a simple box distribution of the ε_1 parameter centred at $\varepsilon_1^0 = 231$ K with the total width $\Delta\varepsilon_1 = 382$ K, and using the values $\Delta = 57$ K and $\rho_0 = 1119\ \mu\Omega$ cm, is displayed as a solid curve in figure 6. This modified KG fit is almost perfect. Here, however, it is important to realize that the fit-determined values of the ε_1^0, $\Delta\varepsilon_1$ and Δ parameters are relatively large, so one could expect to observe magnetic ordering phenomena already at considerably higher temperatures than actually detected in the i-AlPdMn samples of similar resistivity data (i.e. below liquid He temperatures). These values of the obtained fit parameters demonstrate the limited applicability of the KG theory to fit the $\rho(T)$ data away from the low-temperature regime. This is, however, exactly the same problem as encountered in the application of the QIE theory. In addition, the introduction of the distribution of the ε_1 parameter is, from the

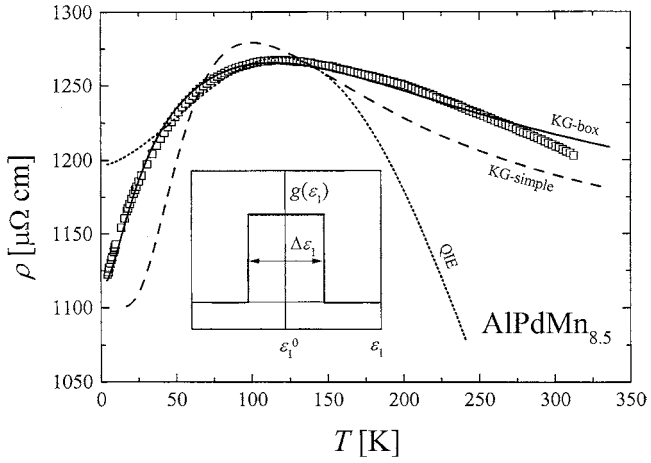

Figure 6. Electrical resistivity of $AlPdMn_{8.5}$. The dashed curve is the simple KG fit with equation (7), whereas the solid curve (denoted as 'KG-box') represents an improved KG fit using a distribution of the ε_1 parameter, $(\rho/\rho_0)^{-1} = \int [\rho(\varepsilon_1)/\rho_0]^{-1} g(\varepsilon_1)\,\mathrm{d}\varepsilon_1$, with $\rho(\varepsilon_1)$ given by equation (7). The rectangular distribution $g(\varepsilon_1)$ centred at $\varepsilon_1^0/k_B = 231$ K with the total width $\Delta\varepsilon_1/k_B = 382$ K is displayed as an inset. An indicative QIE fit (dotted curve) is shown for comparison.

fitting point of view, equivalent to introducing one fit parameter more ($\Delta\varepsilon_1$ in this case). The total number of fit parameters in the KG model then becomes four, which is the same as in the case of the QIE model. The large number of fit parameters in both cases puts ambiguity on the reliability of the models. For comparison we show in figure 6 an attempt to fit the data with the QIE theory. The fit (dotted curve) using parameters $\sigma(0) = 8.4 \times 10^{-4}$ $(\mu\Omega\ \mathrm{cm})^{-1}$, $A = 2.8 \times 10^{-4}$ $(\mu\Omega\ \mathrm{cm})^{-1}$, $T_0 = 230$ K and $p = 3.1$ again fails completely at both low and high temperatures, showing the non-applicability of the QIE model to $\rho(T)$ data with a small NTC above the maximum.

4. Conclusions

The above results yield the following conclusions. From the experimental point of view there exists rather convincing evidence that the maximum in the temperature-dependent resistivity of QCs is a magnetic effect, related either to the intrinsic magnetism of QC structures or to the presence of randomly distributed extrinsic magnetic impurities. The temperature of the $\rho(T)$ maximum is proportional to the concentration of magnetic moments. From the theoretical point of view the situation is much less clear. The KG theory—based on the existence of virtual-bound electronic states at the Fermi level that are formed in the vicinity of 'foreign' atoms in the host metallic matrix—correctly predicts the shift of the $\rho(T)$ maximum to higher temperatures for an increased magnetic moment concentration, hence describing the appearance of the $\rho(T)$ maximum as a magnetic effect. It also predicts a simple NTC $\rho(T) \propto 1/T$ for nonmagnetic impurities, which is the same as the result of the Janot VRH theory. From the quantitative point of view, the KG theory works better for resistivities exhibiting a small NTC above the $\rho(T)$ maximum. The QIE model—that does not consider the $\rho(T)$ maximum as a magnetic effect—acts just the opposite, being more or less perfect for samples with a large NTC resistivity above the maximum and qualitative only for small NTC resistivities. Both theories, however, suffer from similar problems. They involve a large number of fit parameters and were developed under

the assumption of low temperatures, where the phononic contribution to the resistivity can be neglected. When applied to $\rho(T)$ data extending up to room temperature, the fit parameter values consequently become rather unphysical. We believe that—though very simplified and qualitative at the moment—the KG theory can serve as one more step towards a more complete, QC-specific model of the electrical resistivity that would explain the observed $\rho(T)$ maximum in magnetic QCs as a magnetic phenomenon.

Acknowledgment

We thank Dr T J Sato from NIMS Tsukuba for the provision of the CdCa sample.

References

[1] Rapp Ö 1999 *Physical Properties of Quasicrystals* ed Z M Stadnik (New York: Springer) p 127
[2] Fujiwara T 1999 *Physical Properties of Quasicrystals* ed Z M Stadnik (New York: Springer) p 169
[3] Akiyama H, Hashimoto T, Shibuya T, Edagawa K and Takeuchi S 1993 *J. Phys. Soc. Japan* **62** 939
[4] Lanco P, Klein T, Berger C, Cyrot-Lackmann F, Fourcaudot G and Sulpice A 1992 *Europhys. Lett.* **18** 227
[5] Rodmar M, Grushko B, Tamura N, Urban K and Rapp Ö 1999 *Phys. Rev.* B **60** 7208
[6] Escudero R, Lasjaunias J C, Calvayrac Y and Boudard M 1999 *J. Phys.: Condens. Matter* **11** 383
[7] Klein T, Berger C, Mayou D and Cyrot-Lackmann F 1991 *Phys. Rev. Lett.* **66** 2907
[8] Bilušić A, Bešlić I, Ivkov J, Lasjaunias J C and Smontara A 1999 *Fizika* A **8** 183
[9] Gerritsen A N and Linde J O 1952 *Physica* **18** 877
[10] Korringa J and Gerritsen A N 1953 *Physica* **19** 457
[11] Dolinšek J, Apih T, Simsič M and Dubois J M 1999 *Phys. Rev. Lett.* **82** 572
[12] Apih T, Klanjšek M, Rau D and Dolinšek J 2000 *Phys. Rev.* B **61** 11 213
[13] Dolinšek J, Klanjšek M, Apih T, Smontara A, Lasjaunias J C, Dubois J M and Poon S J 2000 *Phys. Rev.* B **62** 8862
[14] Apih T, Plyushch O, Klanjšek M and Dolinšek J 1999 *Phys. Rev.* B **60** 14 695
[15] Mabbs F E and Machin D J 1973 *Magnetism and Transition Metal Complexes* (London: Chapman and Hall) p 7
[16] Van Vleck J H 1952 *The Theory of Electrical and Magnetic Susceptibilities* (Oxford) p 285
[17] Lasjaunias J C, Sulpice A, Keller N, Préjean J J and de Boissieu M 1995 *Phys. Rev.* B **52** 886
[18] Chernikov M A, Bernasconi A, Beeli C, Schilling A and Ott H R 1993 *Phys. Rev.* B **48** 3058
[19] Efros A L and Shklovskii B I 1975 *J. Phys. C: Solid State Phys.* **8** L4
[20] Janot C 1996 *Phys. Rev.* B **53** 181
[21] Janot C and de Boissieu M 1994 *Phys. Rev. Lett.* **72** 1674
[22] Chernikov M A, Bernasconi A, Beeli C and Ott H R 1993 *Europhys. Lett.* **21** 767
[23] Lindqvist P, Lanco P, Berger C, Jansen A G M and Cyrot-Lackmann F 1995 *Phys. Rev.* B **51** 4796
[24] Fukuyama H and Hoshino K 1981 *J. Phys. Soc. Japan* **50** 2131
[25] Lee P A and Ramakrishnan T V 1985 *Rev. Mod. Phys.* **57** 287
[26] Friedel J 1956 *Can. J. Phys.* **34** 1190
[27] Blandin A and Friedel J 1959 *J. Phys. Radium* **20** 160
[28] Lasjaunias J C, Calvayrac Y and Yang Hongshun 1997 *J. Physique* I **7** 959
[29] Yosida K 1957 *Phys. Rev.* **107** 396
[30] Schmitt R W 1956 *Phys. Rev.* **103** 83